# MAGNETIC-FIELD MEASUREMENTS OF SUPERCONDUCTING MAGNETS FOR A HEAVY-ION ROTATING-GANTRY AND BEAM-TRACKING SIMULATIONS

S. Suzuki, Y. Iwata, K. Noda, T. Shirai, T. Furukawa, T. Fujita, K. Shouda, S. Mori,
K. Mizushima, and Y. Hara

National Institute of Radiological Sciences (NIRS), 4-9-1 Anagawa, Inage, Chiba 263-8555, Japan

H. Arai, and T. Fujimoto
Accelerator Engineering Corporation (AEC), 3-8-5 Konakadai, Inage, Chiba 263-0043, Japan

T. Ogitsu
High Energy Accelerator Research Organization (KEK), 1-1 Oho, Tsukuba, Ibaraki 305-0801, Japan

T. Obana
National Institute for Fusion Science (NIFS), 322-6 Oroshi-cho, Toki-city, Gifu 509-5292, Japan

N. Amamiya
Faculty of Engineering, Kyoto University, Kyoto daigaku-Katsura, Nishikyo-ku, Kyoto, Japan

T. Orikasa, S. Takayama, Y. Nagamoto, and T. Yazawa
Toshiba Corporation, 1-1-1 Shibaura, Minato-ku, Tokyo 105-8001, Japan

## Abstract

Manufacture of superconducting rotating-gantry for heavy-ion radiotherapy is currently in progress. This rotating gantry can transport heavy ions having 430 MeV/nucleon to an isocenter with irradiation angles of over 0-360 degrees, and enables advanced radiation-therapy. To reduce the size and weight of the rotating gantry, we designed superconducting magnets that can independently excite dipole and quadrupole field. The three-dimensional scanning-irradiation method is performed in this rotating gantry. Therefore, uniformity of magnetic field is quite important, since scanned beams traverse through these superconducting magnets before reaching to the isocenter.

In the present work, we precisely measured the magnetic-field distributions of the superconducting magnets for the rotating gantry. We used Hall probes to measure the magnetic-flux density. The magnetic-field distributions were determined by measuring Hall voltage, while moving the Hall probes on a rail, which has the same curvature as a center trajectory of beams. The measured-field distributions were compared with designed distributions by using a three-dimensional electromagnetic-field solver, the OPERA-3D code. Furthermore, beam-tracking simulations were performed by using the measured magnetic-field distributions to verify the design of the superconducting magnets.

## INTRODUCTION

In 1993, HIMAC (Heavy Ion Medical Accelerator in Chiba) was built for heavy-ion radiotherapy in National Institute of Radiological Sciences (NIRS). Since the next year 1994, clinical study for cancer treatment has been started. The number of patients have been treated by using HIMAC, exceeds 7000 [1]. This result also shows the validity of heavy-ion radiotherapy to the cancer. Now, some heavy-ion clinical-accelerator facilities are operated in Japan, heavy-ion radiotherapy is becoming widespread. These successful facts led us advance this powerful tool.

Recently, we built the new treatment facility that has three-treatment room [2]. In the two of them, both horizontal and vertical fixed-irradiation port are installed, and the other room is prepared for a rotating-gantry port. Three-dimensional raster-scanning irradiation with a pencil beam is performed in two-fixed port [3-5], and also will be employed for treatment in the rotating-gantry port.

The rotating gantry can irradiate the beam from 0-360 degrees, therefore the patient dose not need to be moved for angle by angle, differently from the radiation treatment with a fixed port. Owing to this, we can perform advanced radiation therapy with the high accuracy of irradiation position. Furthermore, this merit reduces the burden of the patient. Now the manufacture of rotating gantry is proceeding. The rotating gantry will be completed in 2015.

## LAYOUT OF BEAMLINE

The only rotating gantry for heavy-ion therapy exists in Heidelberg Ion-Beam Therapy Center (HIT) [6]. It is reported that, its length is 25 m, and its weight of rotating part is 600 tons. Figure 1 shows the schematic drawing of the beam-line for the rotating gantry developed in NIRS. The beam-line configuration for the gantry mainly consists of ten-bending magnets. To reduce the size and weight of the gantry, we designed superconducting combined functional magnets. Owing to this, the length and the radius of the gantry are 13 m, and 5.5 m, respectively. We expect that the size of this gantry will be same as that of the proton gantry.

In the middle of beam-line, two-normal-conducting scanning magnets are installed. Therefore, the good uniformity of the magnetic field is required for the superconducting magnets at the downstream of the scanning magnets, since scanned beams traverse through these magnets before reaching to the isocenter.
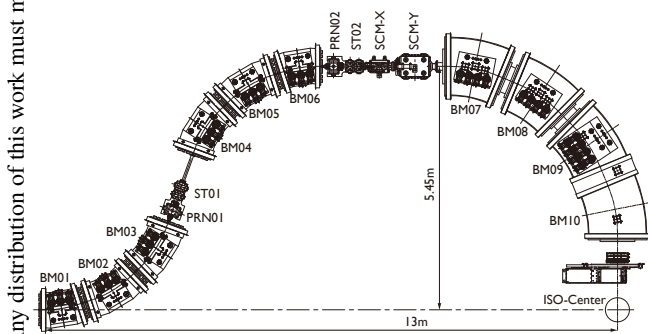


Figure 1: A schematic drawing of the beam-line config-uration for the rotating gantry. The superconducting-bending magnets are shown as BM01-BM10. The scan-ning magnets are shown as SCM-X and SCM-Y.

## MAGNETIC-FIELDE MEASUREMENTS

Recently, we measured the magnetic-field distribution for BM10 that is the last bending magnet. The magnetic flux density was measured by using Hall probes. In order to obtain the field distribution, we measured Hall voltage while moving Hall probes on a rail that was along a center trajectory of the curved magnet. In this method, we can obtain the several distributions for the trajectories in proportion to the number of Hall probes used for the measurement. The Hall voltage has temperature dependence. Accordingly, in offline analysis, we corrected that with temperature information obtained from temperature sensor attached to the Hall probe holder. Moreover, in off-line analysis, we corrected the individual difference of Hall voltages, with the voltage ratio of each Hall probes and a reference probe that were measured in advance. By using this method, the dispersion of Hall voltage was improved by about ten times.

Figure 2 shows the measured magnetic-flux distribution along center trajectory at respective excitation current of the dipole coil. The maximum current 231.2 [A]

corresponds to the $^{12}$C beam energy of 430 [MeV/nucleon], and the lowest current 91.3 [A] corresponds to that of 80 [MeV/nucleon]. We could measure the field distribution in the whole region of a trajectory.

Figure 3 shows the horizontal position dependences of the uniformity of *BL* products. It is clearly observed that the dipole field contains quadrupole component whose *GL* product is approximately -0.034 [T]. As a result, the uniformity of *BL* product is about ten times larger than that of designed value [7]. We do not know this cause clearly. However, we consider that the systematic error in production of the magnet generates the unexpected quadrupole component. Although we have observed that, this obstacle to beam transport can be successfully canceled by exciting the quadrupole filed properly. Fortunately, this superconducting magnet is a combined-functional magnet.

Note that the value at $\Delta x = 0$ deviates from the systematics of the other, because this center probe was used as a reference probe in the voltage ratio measurement. Consequently, the systematic error at $\Delta x = 0$ could be generated, because only this Hall voltage was absolute value, and the other were relative values corrected by using voltage ratio.
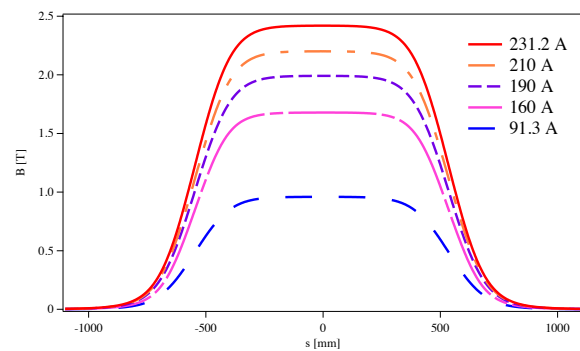


Figure 2: The measured magnetic field along center traject-ory. The color code shows the difference of the excitation current. The length of BM10 is ± 550mm.
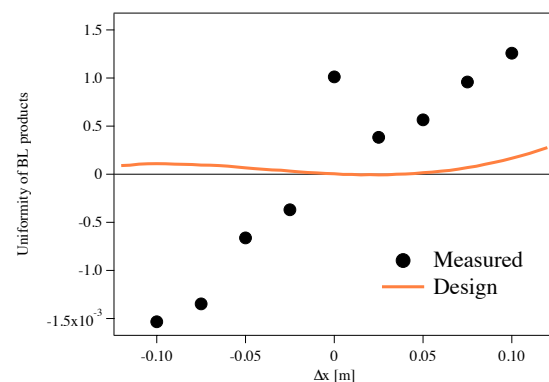


Figure 3: The horizontal position dependences of *BL* products. The solid circles show measured value. The solid line shows designed value calculated by using OPERA-3D code [7]. The dipole current is 231.2 [A].

## BEAM-TRACKING SIMULATIONS

To verify the design of superconducting magnets, we performed beam-tracking simulations by using measured magnetic-field. We simulated the beam tracks from the scanning magnet SCM-Y to the isocenter. The twiss parameter of particles in front of the SCM-Y were determined to be $\beta_x = 9.97$ [m], $\alpha_x = -0.96$, $\beta_y = 13.52$ [m], $\alpha_y = 0.74$, for the matching condition that is represent in Fig. 4. The beam emittance was taken to be $\varepsilon_x = \varepsilon_y = 2$ [$\pi$ mm mrad]. We used the following equation of motion on curvilinear coordinate system,

$$x'' - k(1 + kx) - \frac{dx}{ds}\frac{x'}{1+kx}(2kx' + k'x)$$
$$- \frac{\sqrt{g}}{B\rho}\left\{B_s y' + B_x\frac{x'y'}{1+kx} - B_y\frac{(1+kx)^2 + x'^2}{1+kx}\right\} = 0, \quad (1)$$

$$y'' - \frac{y'}{1+kx}(2kx' + k'x)$$
$$- \frac{\sqrt{g}}{B\rho}\left\{B_s x' + B_x\frac{(1+kx)^2 + y'^2}{1+kx} - B_y\frac{x'y'}{1+kx}\right\} = 0, \quad (2)$$

with $g = x'^2 + y'^2 + (1 + kx)^2$,

where $k = 1/\rho(s)$, The $B\rho$ was adjusted to the measured $BL$ products at the center trajectory of the beams. The $x(s)$ and $y(s)$ were obtained by numerically integration using the 4th order Runge-Kutta method. The magnetic-flux density at which a particle locates, were determined by interpolating nearby those of measured data.

Up to the present, we have not performed magnetic-field measurement of superconducting magnets BM07-BM09, except for BM10, since the manufacture of these superconducting magnets has not finished. Accordingly, we also used the magnetic-field data of BM10 as those of the other superconducting magnet, by assuming that: BM09 has an exactly same specification of BM10, for BM07 and BM08, the apertures of these two superconducting magnets are smaller than that of BM10, thus it could be expected that the field quality of these two magnets is better than that of BM10. In the present simulations, we used data of dipole field at 231.2 [A]. For the quadrupole filed, we used scaled data of quadrupole field at 200 [A], so as to reproduce the calculated beam optics for the matching condition. Under these conditions, we performed beam-tracking simulations for various kick angles given by SCM-X and SCM-Y. Fig. 5 (a) shows the results of the simulations. We can see the distortion for both horizontal axis and vertical axis, respectively. This distortion would be ascribed to the measurement error of magnetic field. The maximum shift from the aimed position was about 9.1 [mm], that corresponds to the correction amount of 7% of the kick angle of the scanning magnet. In Fig. 5 (b), (c), beam spots at the two-location are shown. The difference of the spot size also would be attribute to the measurement error.

Although we have observed the unexpected quadrupole component, beam optics is hardly different from previous design [7]. We concluded that the positions and the size of the beam spot could be under control.
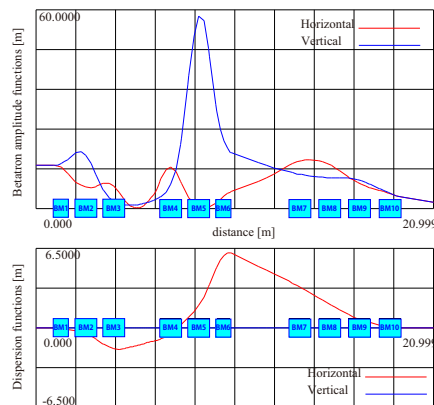


Figure 4: Betatron functions and dispersion functions of the calculated beam optics for the matching condition. In the isocenter, $\beta_x = \beta_y = 2$ [m].
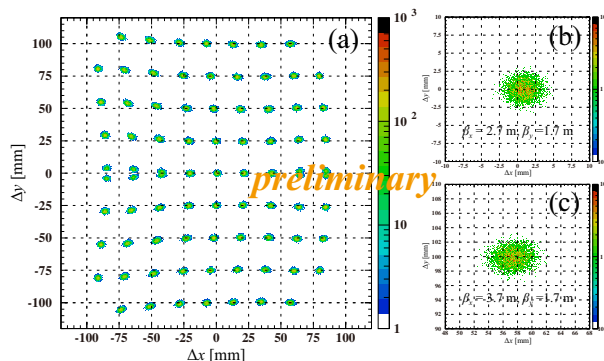


Figure 5: Beam profile at the isocenter calculated by tracking simulations. Each of beam spots was made up of 5000 particles, and the difference of the spots positions was given by respective kick angles of SCM-X ($\pm$ 18 mrad) and SCM-Y ($\pm$ 21 mrad).

## CONCLUSION

Although we have observed the unexpected quadrupole component, we found that the affect is not matter. The most of results are consistent with the design, and satisfactory. We will continue the measurement of the magnetic field for the rest of magnets.

## REFERENCES

[1] T. Kamada, Carbon-Ion Radiotherapy, Springer, 121-123 (2014).

[2] K. Noda, et al., Nucl. Instrum. Meth. Phys. Res., B 266, 2182 (2008).

[3] T. Furukawa, et al., Nucl. Instrum. Meth. Phys. Res., B 266, 2186 (2008).

[4] T. Furukawa, et al., Med. Phys. 34, 1085 (2007).

[5] T. Furukawa, et al., Med. Phys. 37, 5672 (2010).

[6] https://www.klinikum.uni-heidelberg.de/First-heavy-ion-gantry.112987.0.html?&L=1

[7] Y. Iwata, et al., Phys. Rev. S.T. Accel. Beams 15, 044701 (2012).